Oral Delivery of Bioencapsulated Proteins Across Blood–Brain and Blood–Retinal Barriers

Neha Kohli[1], Donevan R Westerveld[1], Alexandra C Ayache[1], Amrisha Verma[2], Pollob Shil[2], Tuhina Prasad[2], Ping Zhu[2], Sic L Chan[1], Qiuhong Li[2] and Henry Daniell[1]

[1]School of Dental Medicine, University of Pennsylvania, Philadelphia, Pennsylvania, USA; [2]Department of Ophthalmology, College of Medicine, University of Florida, Gainesville, Florida, USA

Delivering neurotherapeutics to target brain-associated diseases is a major challenge. Therefore, we investigated oral delivery of green fluorescence protein (GFP) or myelin basic protein (MBP) fused with the transmucosal carrier cholera toxin B subunit (CTB), expressed in chloroplasts (bioencapsulated within plant cells) to the brain and retinae of triple transgenic Alzheimer's disease (3×TgAD) mice, across the blood–brain barriers (BBB) and blood–retinal barriers (BRB). Human neuroblastoma cells internalized GFP when incubated with CTB-GFP but not with GFP alone. Oral delivery of CTB-MBP in healthy and 3×TgAD mice shows increased MBP levels in different regions of the brain, crossing intact BBB. Thioflavin S–stained amyloid plaque intensity was reduced up to 60% by CTB-MBP incubation with human AD and 3×TgAD mice brain sections *ex vivo.* Amyloid loads were reduced *in vivo* by 70% in hippocampus and cortex brain regions of 3×TgAD mice fed with bioencapsulated CTB-MBP, along with reduction in the ratio of insoluble amyloid β 42 ($A\beta_{42}$) to soluble fractions. CTB-MBP oral delivery reduced $A\beta_{42}$ accumulation in retinae and prevented loss of retinal ganglion cells in 3×TgAD mice. Lyophilization of leaves increased CTB-MBP concentration by 17-fold and stabilized it during long-term storage in capsules, facilitating low-cost oral delivery of therapeutic proteins across the BBB and BRB.

Received 2 September 2013; accepted 19 November 2013; advance online publication 7 January 2014. doi:10.1038/mt.2013.273

INTRODUCTION

Drug delivery of biologics from bloodstream to the brain across the blood–brain barrier (BBB) has long been a major challenge to treat neuronal degenerative disorders.[1–3] Invasive approach to bypass the BBB includes intracerebro-ventricular infusion, convection-enhanced delivery, or microchip systems to release such therapeutics. However, these strategies are neither efficient to deliver optimal concentrations of drug to the brain parenchyma, nor patient friendly, enhancing tumor dissemination.[4] Modification of chemical properties of drugs can facilitate penetration across BBB but often results in losing the desired central nervous system (CNS) activity.[2,4] Although the transcytosis mechanism[4] across polarized endothelial cells at BBB is not clear, selection of high-affinity ganglioside M1 (monosialotetrahexosyl) receptor (GM1) binding ligands, like the cholera toxin B subunit (CTB), should address the process of transcytosis across BBB. However, no attention has been paid for developing oral drug delivery systems to address neurological diseases.

Likewise, ocular drug delivery, particularly to the posterior segment of the eye, is also a major challenge due to several anatomical and physiological constrains of the eye.[5,6] Topically administered drug cannot reach the retina and vitreous cavity because of the ocular surface barriers, which include cornea epithelium, stroma, and endothelial layers, continuous tear drainage, frontward flow of aqueous humor, and surrounding blood circulations, all limiting the penetration of topically administered drug. Although intravenous administration is extensively used for delivering drugs to the posterior part of the eye, ocular pharmacologists face major obstacles[7] such as retinal detachment, endophthalmitis, and high intraocular pressure through this accessible route.

Alzheimer's disease (AD) is the most common neurodegenerative disease and the sixth leading cause of death in the United States, affecting an estimated 5.4 million Americans and 36 million people globally,[8] with treatment cost exceeding US$600 billion, posing a major health-care challenge. By the year 2050, it is estimated that the incidence of AD will reach >100 million patients worldwide.[9] One of the major pathological hallmarks of AD is the deposition of amyloid β 42 ($A\beta_{42}$) as extracellular neuronal plaques.[10] The $A\beta_{42}$ peptide is produced by the sequential cleavage of amyloid precursor protein within lipid rafts by endoproteolytic enzymes β and γ secretase, respectively.[11] Following the cleavage of amyloid precursor protein, Aβ fragments of different lengths $A\beta_{42}$, $A\beta_{38}$, and even $A\beta_{46}$ are produced, with the predominant form being $A\beta_{40}$.[12] Although $A\beta_{42}$ is a minor species, it has a greater propensity to aggregate and form plaques. This leads to a detrimental loss of synaptic structural integrity/communication between axon and dendrites, contributing to cognitive dysfunction leading to neuronal degeneration.[13] Current US Food and Drug Administration–approved pharmacotherapies provide some symptomatic benefits, but they do not prevent disease progression.[14]

Furthermore, visual abnormalities are also prevalent among AD patients. Visual disturbances in AD patients include impaired motion and depth perception, spatial contrast sensitivity and color recognition,[15] associated with degeneration and loss of retinal

Correspondence: *Henry Daniell, School of Dental Medicine, University of Pennsylvania, 240 South 40th Street, Philadelphia, Pennsylvania 19104-6030, USA. E-mail: hdaniell@upenn.edu*

ganglion cells (RGCs) and reduction of retinal nerve fibers.[16] Aβ deposition in the retina appeared to be associated with RGC apoptosis and retinal structural and functional impairment.[16] In addition, Aβ deposits have been reported in glaucomatous optic nerve heads, drusen of age-related macular degeneration, and lens with cataracts.[17–20] Intravitreal injection of Aβ causes RGC damage, illustrating Aβ toxicity to retinal tissue.[21] Therefore, for diagnosis of AD, retinal scans have been used to identify Aβ plaque deposits.

Recently, the US Food and Drug Administration approved a carrot cell–based system for production of the first human therapeutic protein.[22] Oral delivery of chloroplast-derived therapeutics bioencapsulated in plant cells eliminates the need for expensive fermentation, purification, cold storage and transportation, and sterile delivery.[23] Bioencapsulation of therapeutic proteins by plant cell wall ensures their protection from proteolytic degradation in the stomach and facilitates their delivery to the circulatory system by the action of commensal microbes and receptors present in the gut.[23] The delivery of fusion proteins across intestinal epithelium is facilitated by transmucosal carrier, CTB by binding to the ganglioside receptor.[24] Here we report for the first time, the oral delivery of bioencapsulated reporter and therapeutic proteins across BBB and blood–retinal barriers (BRB).

Myelin basic protein (MBP), a major structural protein of CNS comprising ~30% of the total myelin protein, is essential for the formation of CNS myelin,[25] contributing to the stability and maintenance of the sheath. In the early stages of AD, focal demyelination associated with Aβ plaques in white matter is observed in both human tissue and relevant murine models but not in plaque-free areas.[26] Moreover, MBP has also been shown *in vitro* to possess intrinsic protease activity capable of degrading Aβ amyloid and the ability to bind Aβ amyloid and inhibit Aβ fibril formation.[27,28] Bioencapsulated MBP fused with CTB is hypothesized to cross the BBB *in vivo* and degrade Aβ aggregates. Therefore, in this study, we investigate oral delivery of bioencapsulated CTB-MBP in mouse or human brains with advanced AD for delivery across BBB and BRB.

RESULTS

Characterization of CTB-MBP protein expressed in chloroplasts

The CTB-MBP construct is based on the plasmid (Lee/Daniell) (pLD) vector with *trnI-trnA* flanking sequences to facilitate homologous recombination,[29] and the gene of interest is regulated by the psbA promoter and 5′ untranslated region to achieve high-level expression. In the fusion construct, glycine–proline–glycine–proline hinge prevented steric hindrance between two proteins, psbA 3′ untranslated region provided transcript stability, the aadA gene and ribosome binding site conferred spectinomycin resistance for selection (**Figure 1a**). Transplastomic plants were produced through particle bombardment as described earlier.[30] Transplastomic lines were confirmed by Southern blots conferring site-specific integration of transgene into the spacer region between *trnI* and *trnA* genes. Digestion of untransformed wild type (WT) plant DNA with AflIII showed 4.2-kb fragment after hybridizing with ^{32}P-labeled *trnI-trnA* flanking probe, and transplastomic CTB-MBP lines showed only the 6.7-kb fragment, confirming homoplasmy and site-specific integration of transgene (**Figure 1b**). Immunoblots probed with CTB (**Figure 1c**) and MBP (**Figure 1d**) antibody showed ~28.5-kDa fusion protein monomer, dimer at ~57 kDa, and trimer at ~86 kDa in CTB-MBP transplasomic lines. Fresh leaves expressed up to 2% of total leaf protein, but a 17-fold enhanced antigen concentration was achieved by lyophilization of the plant material (**Figure 1c**). Equal loading of protein showed a significant difference in accumulation of CTB-MBP between fresh and lyophilized materials (**Figure 1e**). Moreover, immunoblots probed with CTB antibody showed that lyophilized material maintained stability at room temperature (RT) and protection from degradation over 7 months of storage (**Figure 1f**).

The functionality of CTB-MBP fusion protein was evaluated by GM1 enzyme-linked immunosorbent assay (ELISA), where the ability of CTB to bind to GM1 receptors depends on its pentameric form. GM1 binding assay showed that pentamers of fresh weight and lyophilized CTB-MBP were formed, confirming proper folding and disulfide bond formation (**Figure 1h**). Non-reducing native polyacrylamide gel electrophoresis immunoblots probed with CTB antibody further confirmed the formation of the pentameric structure (**Figure 1g**) within transgenic chloroplasts, attesting functionality of CTB-MBP for *in vivo* studies. Lyophilization process preserved the folding and disulfide bonds of CTB-MBP protein even after prolonged storage at RT (**Figure 1f**).

Oral delivery of bioencapsulated CTB-GFP and CTB-MBP across BBB/BRB

Oral gavage of CTB-green fluorescent protein (GFP) bioencapsulated plant cells created in a previous study[24] showed GFP fluorescence in mouse circulation system. Healthy C57BL/6J mice showed uptake of GFP in the sera and different organs (**Figure 2a**) measured by using GFP ELISA kit. After 2 hours of gavage, 364 pg/ml of GFP was observed in the sera, and a lot more in other organs, showing very efficient and rapid delivery into the circulatory system. The highest GFP retention (2,512 pg/mg) was observed in the liver, followed by the lung (1,720 pg/mg), the kidney (1,446 pg/mg), and the heart (509 pg/mg). A concentration of 348 and 945 pg/mg of GFP uptake in the brain and retinal tissue of mice, sacrificed after 5 hours of the last gavage, shows delivery of GFP across the BBB and BRB in healthy mice having fully intact BBB/BRB. Healthy mice orally gavaged with bioencapsulated CTB-MBP plant leaf material for 3 consecutive days showed MBP deposits in the hippocampus region when evaluated by immunofluorescence on fixing brain tissue overnight (**Figure 2b**). WT and triple transgenic (3×Tg) AD mice fed with CTB-MBP also showed increased MBP levels in different regions of the brain (**Figure 2c–f**), confirming efficient transmucosal delivery of bioencapsulated proteins across the BBB. Data for absolute values are provided along with percentage of respective control samples. The absolute fluorescence intensity values of MBP from WT mouse brain are different from 3×TgAD mice because they are different mouse strains and different in their age. In addition, these experiments were done differently: 3 consecutive days of oral gavage of 6-week-old C57BL/6J mice with CTB-MBP, and sections were freshly cut and immune stained. On the other hand, 15-month-old 3×TgAD mice were gavaged for 3 months, and sections tissues were stored in a freezer for evaluation.

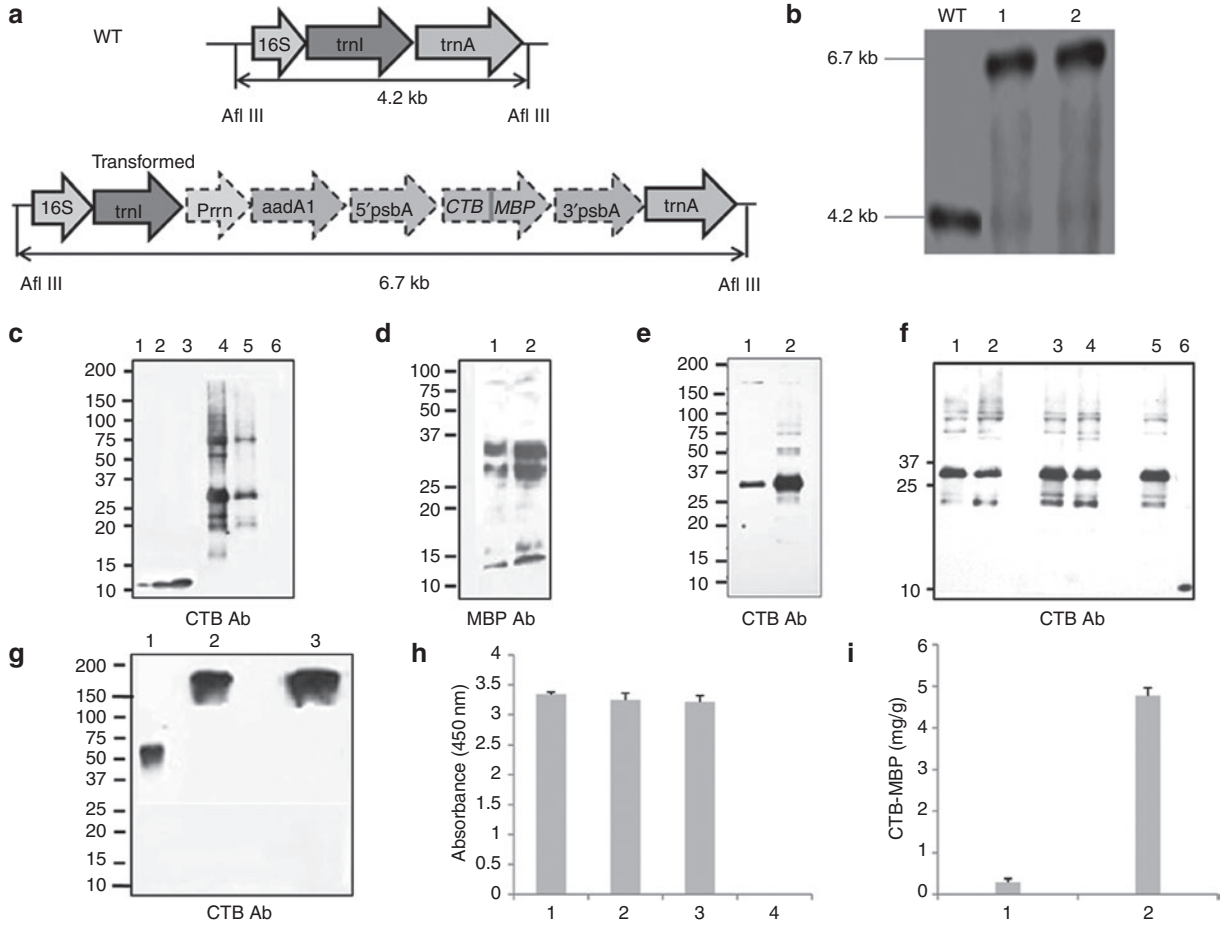

Figure 1 Characterization of CTB-MBP transplastomic lines. (**a**) Schematic representation of wild type (WT) and transformed tobacco chloroplast genome. (**b**) Digestion with AflIII yields 4.2 and 6.7 kb fragments in WT and transplastomic lines,[1,2] respectively in Southern blot. Western blots of CTB-MBP expression in fresh (F) and lyophilized (L) transgenic plant extracts. (**c**) Sodium dodecyl sulfate-polyacrylamide gel electrophoresis (SDS-PAGE) with anti-CTB antibody (Ab). Lanes 1, 2, and 3—12.5, 25, and 37.5 ng purified CTB standard; lanes 4, 5, and 6—20 µg of crude extract F, L, and WT. (**d**) SDS-PAGE with anti-MBP Ab. Lanes 1 and 2—20 µg of F and L, respectively. (**e**) SDS-PAGE with anti-CTB Ab for normalization of F and L transgenic plant proteins. In lanes 1 and 2, equal quantities (100 mg) of F and L samples were ground in 300 µl of extraction. (**f**) Western blot analysis showing long-term stability of CTB-MBP (L) after storage at room temperature (RT) for 7 months. Lanes 1, 2, 3, 4, and 5 (November, January, March, April, and May)—20 µg of L stored at RT for different durations, lane 6—12.5 ng CTB standard. (**g**) Native PAGE probed with anti-CTB Ab. Lane 1—37.5 ng purified CTB standard; lanes 2 and 3—2 µg of F and L, respectively. (**h**) GM1 enzyme-linked immunosorbent assay of purified CTB (25 ng), transgenic CTB-MBP protein in 20 µg of F, L, and WT extracts in lanes 1, 2, 3, and 4 respectively. (**i**) Quantification of CTB-MBP protein (mg of protein/g of total leaf) in F and L plant extracts in lanes 1 and 2, respectively. CTB, cholera toxin B subunit; MBP, myelin basic protein.

Role of CTB in delivery of GFP into M17 human neuroblastoma cells

M17 human neuroblastoma cells[31] incubated with GFP or CTB-GFP showed GFP fluorescence on the surface or within cells only with CTB-GFP and not with GFP alone (**Figure 3a**). The absence of GFP within neuroblastoma cells shows the requirement for CTB as a carrier to deliver the fused protein across CNS cells. Inability of controls, particularly incubation with GFP without CTB fusion, to bind to M17 cells confirms that human neuroblastoma cells can uptake only the CTB-GFP fusion protein.

Ex vivo reduction of amyloid levels in 3×TgAD mice brains by CTB-MBP

Ex vivo studies of Thioflavin S (ThS)–stained brain sections from 24-month-old 3×TgAD mice showed reduction in amyloid plaques in hippocampus and cortex in a concentration-dependent manner when incubated with chloroplast-derived CTB-MBP (**Figure 4a**). Reduction in ThS fluorescence up to 60% was detected after 2 days of incubation with different concentrations of CTB-MBP plant-derived protein, in adjacent brain sections (**Figure 4b**). Incubations with protein extract from WT plants, phosphate-buffered saline (PBS), or purified CTB under identical conditions did not show any effects in ThS intensity, suggesting that CTB-MBP, at an optimal concentration of 50 µg/section, is able to perform Aβ degrading enzymatic activity,[27] thereby reducing their ThS fluorescence (**Figure 4b**). Data shown are mean ± SD of values obtained from 7 adjacent sections and evaluated from a total of 63 fluorescence images, confirming reproducibility of this observation.

Ex vivo reduction of amyloid levels in postmortem human AD brains by CTB-MBP

Ex vivo studies of ThS-stained brain sections of postmortem human brain tissues from advanced AD patients were conducted

with incubation of 50 µg/section CTB-MBP chloroplast expressed protein (**Figure 5a**), **a** working concentration of MBP from *ex vivo* mice brain studies. Incubation with CTB-MBP showed up to 47% ThS fluorescence reduction of stained amyloid plaques in inferior parietal cortex of human brain sections (**Figure 5b**) when compared with WT plant extract, indicating that MBP through its serine proteinase activity is able to degrade amyloid aggregates, thereby reducing their ThS fluorescence (**Figure 5b**) in human brain tissues. Data shown are mean ± SD of values obtained from 5 sections of 5 different human AD postmortem brains and evaluated from a total of 10 fluorescence images. Although only limited human brain tissues were available for this study, we should point out reproducibility of these observations in brain tissues derived from five different individuals. It should be possible to achieve higher percentage of reduction in amyloid aggregates by further increasing concentration of CTB-MBP in *ex vivo* studies.

In vivo reduction of amyloid levels in 3×TgAD mice brain after oral delivery of bioencapsulated CTB-MBP

The effect of oral delivery for a period of 3 months with either the bioencapsulated CTB-MBP, WT plant cells or unfed was evaluated in brain sections of 3×TgAD mice, which were 13–15 months old

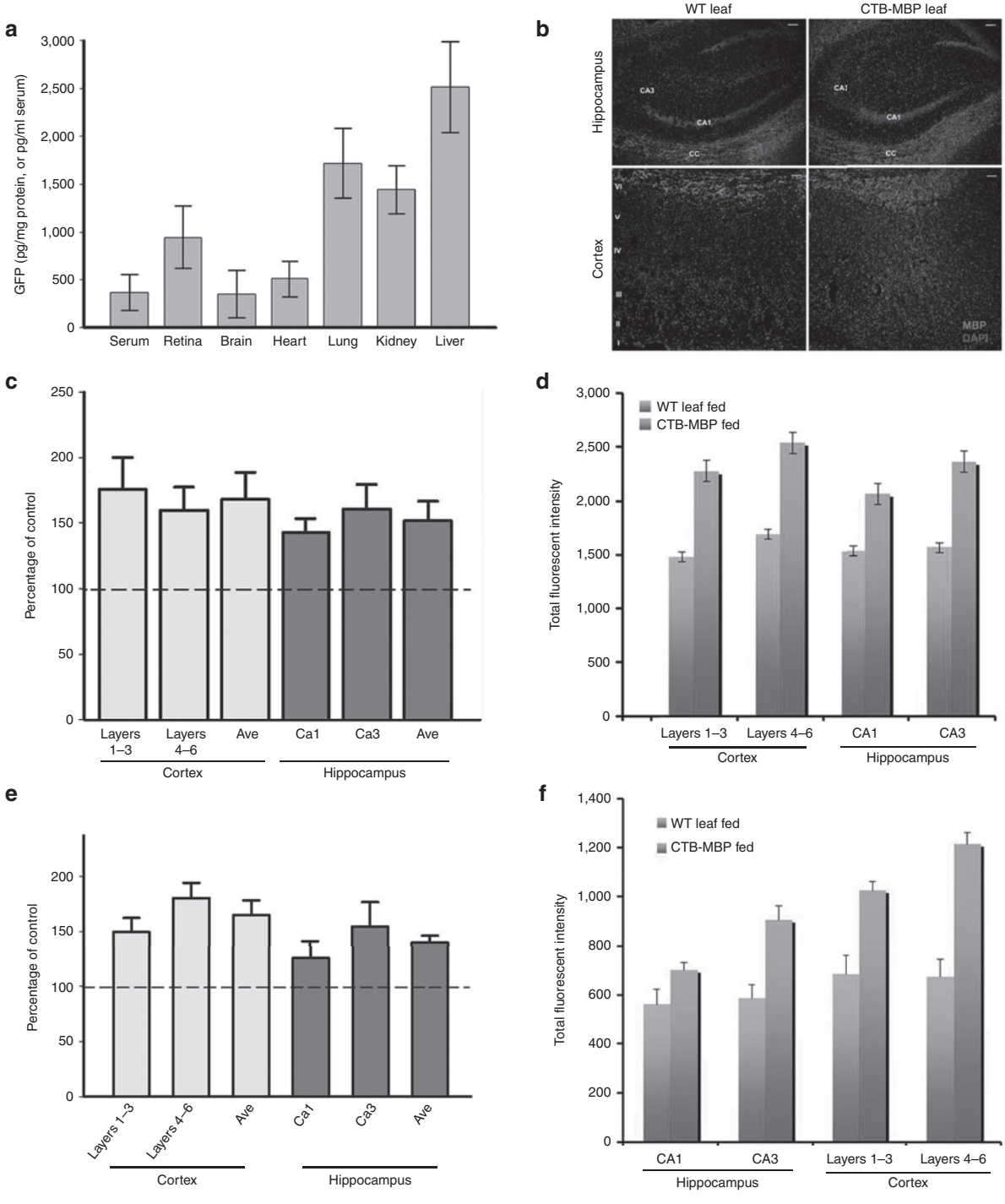

Figure 2 Evaluation of green fluorescent protein (GFP) and myelin basic protein (MBP) levels on oral delivery of plant cells expressing CTB fusion proteins. (**a**) GFP levels in different organs following oral gavage of CTB-GFP leaf material. Six weeks old mice were orally fed with CTB-GFP transgenic tobacco leaf suspension (~ 200 mg/mouse/day; $n = 5$) for 3 consecutive days. Blood samples were collected at 2 and 5 hours after the last gavage at which, mice were sacrificed and tissue samples were collected. GFP concentration in tissues was measured by enzyme-linked immunosorbent assay. (**b**) Immunofluorescent detection of MBP in different regions of the C57Bl/6J mouse brain fed with CTB-MPB or control untransformed (wild type (WT)) leaf materials. WT C57 mice were orally gavaged with CTB-MBP or WT leaf materials for 3 consecutive days. Tissues were harvested 5 hours after the last gavage and fixed overnight in 4% paraformaldehyde. Cryostat brain sections at the level of hippocampus were cut and mounted on Superfrost Plus slides. The sections were incubated in blocking solution (5% bovine serum albumin (BSA) + 0.3% Triton X-100 in phosphate-buffered saline (PBS)) for 1 hour, followed by incubation with rabbit anti-MBP polyclonal antibody 1:100 (ab 65988; Abcam), which recognizes both human and endogenous mouse MBP, overnight at 4 °C. The sections were then incubated with an anti-rabbit immunoglobulin G secondary antibody conjugated to Alexa 594 (Molecular Probes/Invitrogen) for 1 hour at RT. Sections were washed in PBS containing the nuclear counterstain DAPI (4′,6 diamidino-2-phenylindole) and mounted in Dako mounting media (bar = 50 µm). I–VI: six layers of cortex. cc: corpus callosum. (**c**,**d**) Quantification of MBP levels in different regions of C57Bl/6J mouse brain fed with CTB-MPB or control WT leaf materials. Immunofluorescence images were taken from fields within motor cortex (layers 1–3 and layers 4–6) and in CA1 and CA3 regions of hippocampus with a 40× objective and constant exposure times on a Keyence confocal microscope. Threshold for images were set manually using NIH Image J software, and fluorescence intensity was determined by using the measure module. Fluorescent intensity values in CTB-MBP–fed mice were normalized to the control (WT leaf fed) levels. $n = 5$. (**e**,**f**) Quantification of MBP levels in different regions of triple transgenic Alzheimer's disease (3×TgAD) mice brain fed with CTB-MPB or control WT leaf materials for 3 months. The values on *y*-axis of **c** and **e** represent the percentage of the control. $n = 8$. $P < 0.01$ (CTB-MBP versus WT) for all regions measured. AD, Alzheimer's disease; CTB, cholera toxin B subunit; NIH, National Institutes of Health.

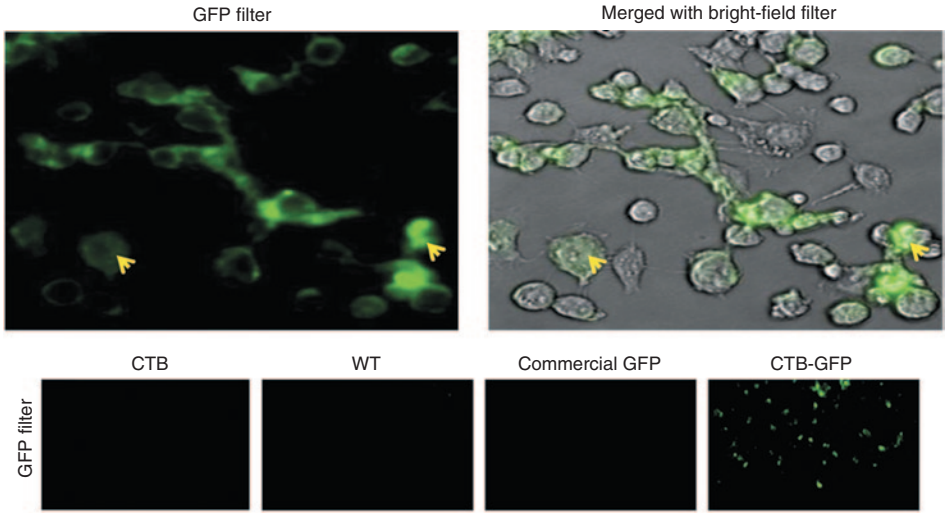

Figure 3 Evaluation of green fluorescent protein (GFP) in M17 human neuroblastoma cells incubated with GFP or CTB-GFP by fluorescence microscopy. CTB-GFP was partially purified from transgenic leaf extracts. M17 cells were incubated with 23.3 nmol/l of CTB alone or WT leaf extracts or purified GFP or CTB-GFP for 24 hours and processed for GFP fluorescence in parallel. Images of live nonfixed cells were taken at an original magnification of ×20 using GFP filter for 4 seconds using Nikon Eclipse, TE2000-E fluorescence microscope. Representative images are shown in the bottom panel. Representative images of intracellular (arrowhead) GFP fluorescence in M17 cells treated with CTB-GFP are also shown. CTB, cholera toxin B subunit; PBS, phosphate-buffered saline.

at the start of this study. Adjacent cortex and hippocampus sections of control and CTB-MBP–treated mice stained with the anti-β-amyloid antibody (**Figure 6a**, red) or ThS (**Figure 6b**, green) were examined and quantified as described in the Methods section. Most plaques were found in the hippocampus region, particularly dentate gyrus (DG), Cornu Ammonis (CA)1, and CA3 sites, from where they started diffusing to the cortex as AD progressed. Aβ level reduction up to 67.3 and 33.4% was observed in hippocampus and cortex, respectively (**Figure 6c**), through immunostaining with anti-Aβ antibody on oral delivery of CTB-MBP. Data shown are mean ± SD of values obtained from 5 adjacent sections from each mouse and evaluated from a total of 120 fluorescence images.

Evaluation of amyloid levels *in vivo* in 3×TgAD mice brain

ThS-stained plaque number and fluorescence intensity was also reduced up to 70 and 40%, respectively (**Figure 7a**), quite consistent across eight groups of age-matched 3×TgAD mice on oral delivery of CTB-MBP leaf material. Data were obtained as described before. Aβ peptide is produced in the brain where it normally remains in a soluble state, and its function is still largely unknown. Accumulation, aggregation, and deposition of Aβ peptides are pathological hallmarks in the AD brains and are found in the insoluble state.[32]

Therefore, we investigated the effect of MBP on Aβ-42 levels from soluble and insoluble fractions of protein extracts isolated from hippocampus of CTB-MBP–fed and control 3×TgAD mice by both ELISA and western blotting using anti-Aβ42–specific antibody. The high molecular weight Aβ-42 aggregates were reduced in the insoluble fractions of hippocampus with corresponding increase of Aβ-42 in the soluble fraction in mice fed with bioencapsulated CTB-MBP, when compared with unfed or WT fed mice (**Figure 7b**,**c**). The ratio of Aβ-42 levels in the insoluble versus soluble fractions of proteins isolated from hippocampus,

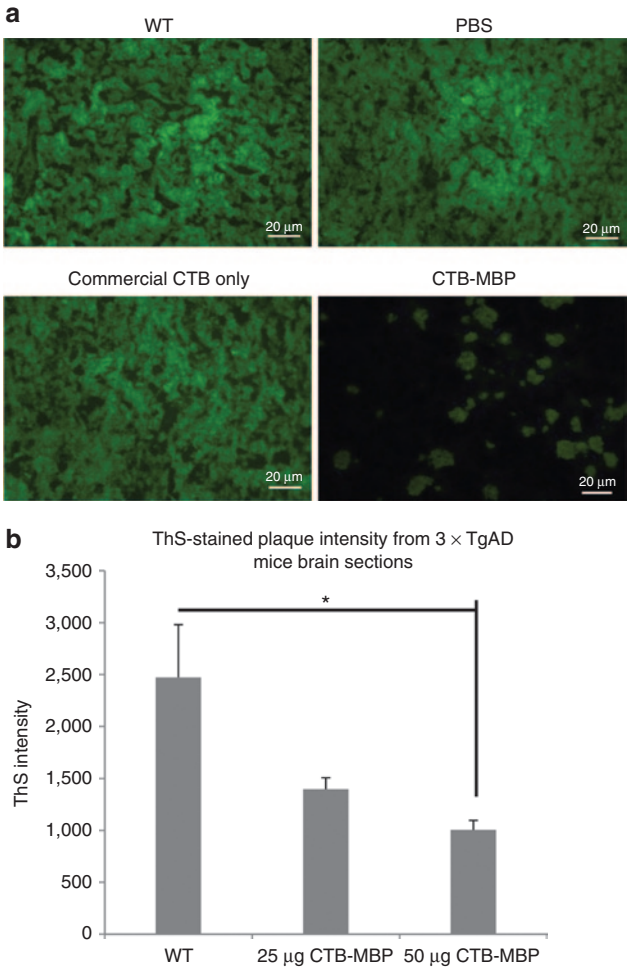

Figure 4 *Ex vivo* evaluation of amyloid plaque load in triple transgenic Alzheimer's disease (3×TgAD) mouse brain tissue sections. (**a**) Sagittal serial sections of brains from 3×TgAD mice were incubated with 25 or 50 μg recombinant CTB-MBP protein purified from transgenic leaf extracts or 25 or 50 μg commercially available purified CTB for 2 days and then stained with 0.02% thioflavin S (ThS) solution to visualize the central dense core of compact amyloid (green) by fluorescence microscopy. As controls, adjacent sections were incubated with 25 or 50 μg of wild type (WT) leaf extracts or saline alone and processed for ThS staining in parallel. Sections including the hippocampus and cortex of representative 24-month-old 3×TgAD mice (bar = 20 μm) are shown. (**b**) Quantification of the relative amounts of amyloid plaque load in the ThS-stained sections after incubation with the indicated proteins or saline alone as described in (**a**). The mean plaque counts in the DG, CA1, and CA3 hippocampal and cortical regions per section (in cortex, mantle, and pallium regions) were determined with NIS Elements for Advanced Research. The values in the histogram represent the mean ± SD> $n = 63$; *$P < 0.05$ (single factor analysis of variance) relative to control. AD, Alzheimer's disease; CTB, cholera toxin B subunit; MBP, myelin basic protein.

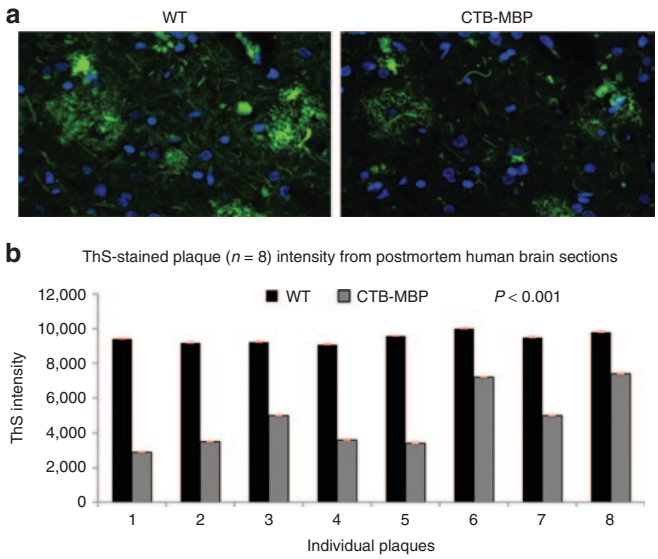

Figure 5 *Ex vivo* evaluation of amyloid plaque load in postmortem Alzheimer's disease (AD) human brain tissue sections. (**a**) Sections of the parietal cortex from human AD were incubated with 50 μg recombinant CTB-MBP protein partially purified from transgenic leaf extracts or 50 μg of partially purified wild type (WT) for 2 days and then stained with 0.02% thioflavin S (ThS) solution to visualize the central dense core of compact amyloid (green) and with DAPI (4′,6 diamidino-2-phenylindole) to identify cell nuclei (blue) by fluorescence microscopy. (Bar = 20 μm). (**b**) Quantification of the relative amounts of amyloid plaque load in the ThS-stained sections after incubation with the indicated proteins as described in (**a**). The mean plaque counts per section were determined with NIS Elements for Advanced Research. The values in the histogram represent the mean ± SD> $n = 8$; *$P < 0.001$ (single factor analysis of variance) relative to control. CTB, cholera toxin B subunit; MBP, myelin basic protein.

measured by ELISA, showed a 2.7-fold decrease (**Figure 7d**) in CTB-MBP–fed mice when compared with respective controls.

Reduction of amyloid level and protection of retinal ganglion cells in mouse retina after oral delivery of bioencapsulated CTB-MBP

In addition to cognitive and behavioral deficits, visual abnormalities are also frequently seen in AD patients. Therefore, we examined the 3×TgAD mouse eyes from animals that received oral gavage of bioencapsulated CTB-MBP plant leaf material for 3 months as well as eyes from age-matched untreated 3×TgAD and healthy mice. Amyloid deposit in the retina was evaluated by immunofluorescence using a biotin-labeled monoclonal antibody specific for Aβ1–42. Intense staining for Aβ1–42 was detected in the inner retina, primarily in the RGC layer in 3×TgAD mice, but almost undetectable in healthy and 3×TgAD mice fed with CTB-MBP leaf materials (**Figure 8a–f**). The retinal level of Aβ1–42 was also evaluated by western blotting using the same antibody, and there was more than 60% reduction in the retinae from CTB-MBP–fed mice, especially among high molecular weight peptide aggregates (**Figure 8g,h**). The retinae of 3×TgAD mice also showed marked loss of RGCs and increase of apoptotic cells detected by TUNEL (terminal dUTP nick end labeling) assay compared with age-matched control mice (**Figure 8i–m**). Amyloid deposit and apoptotic cells are significantly reduced in mice fed with CTB-MBP, and the loss of RGCs was restored.

DISCUSSION

Results of investigations show efficient *in vivo* oral delivery of chloroplast expressed CTB fusion proteins across BBB and BRB. The native confirmation of CTB pentamers facilitates binding to the intestinal GM1 receptors and releases the fused protein to the circulatory system when orally administered. The mechanism of

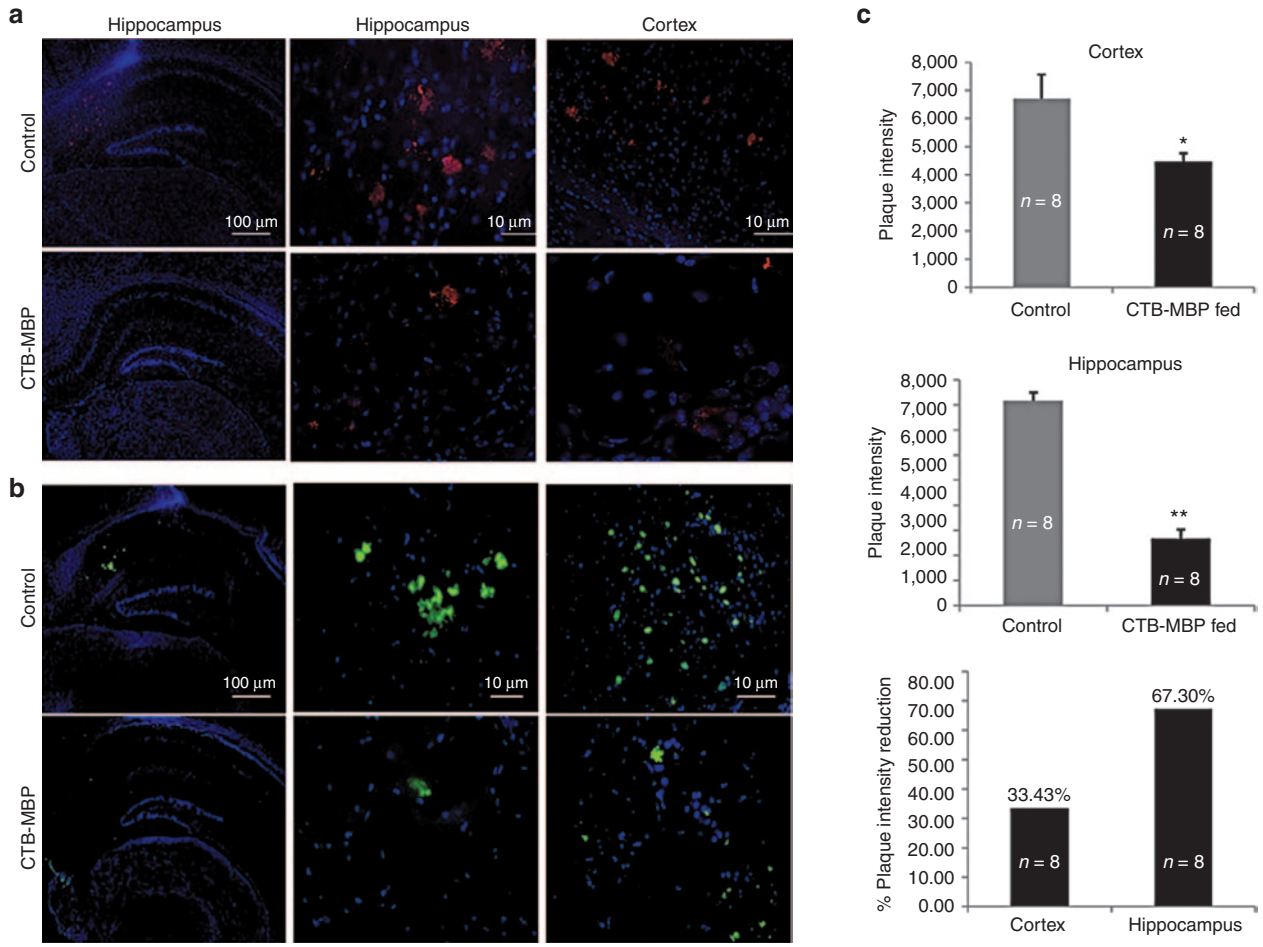

Figure 6 ***In vivo*** **evaluation of amyloid plaque load on orally delivered CTB-MBP in triple transgenic Alzheimer's disease (3×TgAD) mice.** (**a**,**b**) Representative images of the cortical and hippocampal brain sections of 12- to 14-month old 3×TgAD mice fed with either recombinant CTB-MBP bioencapsulated in plant cells (31.2 µg/300 µl/day; $n = 8$ mice), wild type (WT) leaf extracts (300 µl/day; $n = 4$ mice), or unfed ($n = 4$ mice). Sections were stained for amyloid plaques with either anti-Aβ antibody 2454 (red fluorescence; **a**) or thioflavin S (ThS) (green fluorescence; **b**) and with DAPI ((4′,6 diamidino-2-phenylindole) blue) to label cell nuclei. Bar = (i) hippocampus 100 µm and (ii) 10µm at different magnifications and (iii) cortex 10 µm). (**c**) Quantification of the relative amounts of amyloid plaque load in the anti-Aβ and ThS-stained sections from the animals fed with CTB-MBP or WT protein extracts as described in (**a**,**b**). The mean plaque counts in the DG, CA1, and CA3 hippocampal and mantle and pallium cortical regions per section were determined with NIS Elements for Advanced Research. The values in the histogram represent the mean ± SD> n= 63; single factor analysis of variance *$P < 0.05$ for cortex, **$P < 0.01$ for hippocampus when compared with mice treated with WT leaf extracts and unfed. AD, Alzheimer's disease; CTB, cholera toxin B subunit; MBP, myelin basic protein.

CTB binding to GM1 is well known.[33] A recent study has shown that polymeric nanoparticles coated with GM1 binding peptide promoted transcytosis across the BBB.[34] Presence of a voltage-independent GM1 associated with a Ca^{2+} channel has also been observed using CTB-induced Ca^{2+} influx in neuroblastoma cells.[31] Direct evidence for crossing of BBB or BRB by CTB fusion proteins has been provided in our study by: (i) entry of CTB-GFP but not of GFP into neuroblastoma cells; (ii) presence of GFP in brain tissues on oral delivery of CTB-GFP; (iii) increase in MBP in brain tissues on oral delivery of CTB-MBP; (iv) decrease in amyloid plaques in 3×TgAD mouse brain slices in *ex vivo* studies with CTB-MBP incubation with ThS staining; (v) decrease in individual amyloid plaques in human Alzheimer's brain slices in *ex vivo* studies with CTB-MBP incubation with ThS staining; (vi) decrease in amyloid plaques in 3×TgAd mouse brain on oral delivery of CTB-MBP bioencapsulated in plant cells (ThS staining and immunofluorescence images and quantitation); and (vii) removal of Aβ plaques in 3×TgAd mouse retina on oral delivery of CTB-MBP. All these independent lines of investigations provide direct evidence for CTB fusion proteins crossing BBB and BRB, the key finding of this research project.

When compared with significant GFP delivery observed in the brains of healthy mice with intact BBB, the amount of CTB fused protein delivered across impaired BBB in AD brains is anticipated to increase further. BBB impairment is associated with more rapid progression in AD.[35] Previous literature[27,28] has shown that MBP inhibited Aβ fibril formation, where binding site for Aβ is situated at N-terminal 64 amino acids of MBP. Inhibition of fibril assembly by N-terminal domain of MBP was observed. MBP may directly degrade Aβ peptide aggregates/plaques[36] due to its intrinsic proteinase activity as also shown in our *ex vivo* studies. MBP may prevent Aβ peptide aggregation and plaque formation by direct binding of MBP through its N-terminal domain.[27] It is likely that both mechanisms may take place, because a substantial fraction

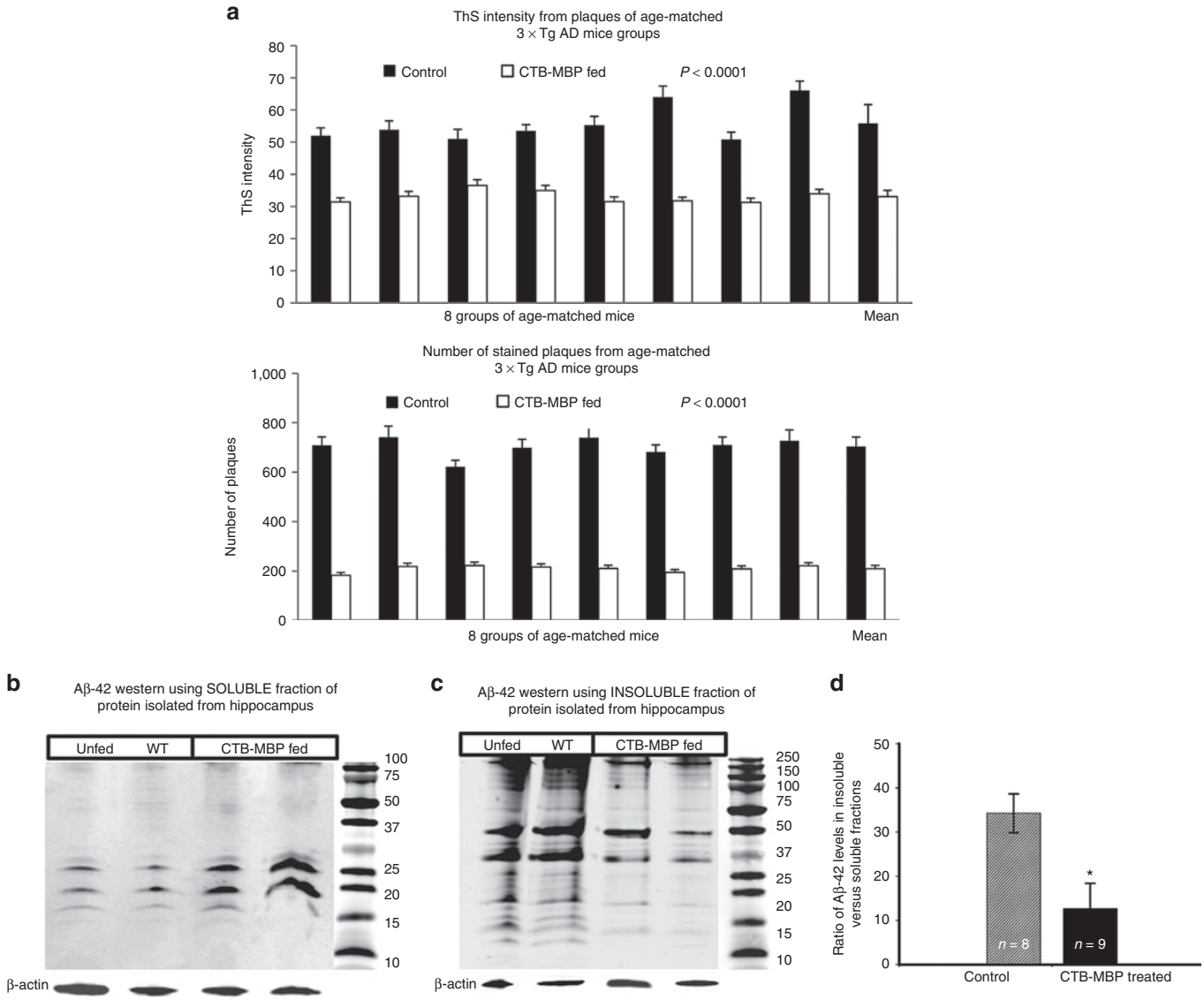

Figure 7 Quantitative evaluation of amyloid levels in triple transgenic Alzheimer's disease (3×TgAD) mice on CTB-MBP oral delivery. (**a**) Eight groups of age-matched 3×TgAD mice fed with CTB-MBP showed consistent reduction in thioflavin S (ThS) intensity stained amyloid plaques, ***$P < 0.0001$, evaluation of (**b**–**d**) total Aβ(40/42) levels were measured by immunoblotting using anti-Aβ42 antibody, 12F4 (**b**,**c**) and enzyme-linked immunosorbent assay (**d**). *$P < 0.05$. AD, Alzheimer's disease; CTB, cholera toxin B subunit; MBP, myelin basic protein; WT, wild type.

of the fusion protein will likely be cleaved in the circulation, as well as at target cells on uptake. Our data show increased MBP levels in different regions of the brain from animals fed with CTB-MBP; however, this detection method is not sensitive enough to differentiate internalized versus extracellular MBP protein. Our results clearly demonstrate the uptake of CTB-MBP into different regions of the brain via oral delivery of the protein bioencapsulated in plant cells. Future studies will be needed to fully understand molecular and cellular mechanism of this process.

It is well known that ThS staining is specific for AB-immunoreactive deposits in the brain, and computer algorithms to detect such neurons have been developed.[37] This study also shows significant reduction of ThS-stained amyloid deposits in advanced human AD post mortem brain sections, when incubated with CTB-MBP. However in each brain section, obtained from different individuals suffering with AD at an advanced stage, consistent reduction of ThS staining was observed on incubation with chloroplast-derived CTB-MBP. Similarly, we observed significant concentration-dependent degradation and/or reduction of amyloid levels in the brains of old 3×TgAD mice on CTB-MBP incubation. We observed that 3×TgAD mice brain showed a significant decrease of amyloid levels when fed with CTB-MBP, particularly in dentate gyrus, CA1 and CA3 regions of hippocampus, and in cortical brain regions, which are known to carry the most amyloid burden in transgenic AD mice as well as in human AD.[38] Moreover, ThS-positive amyloid deposits were observed in the areas of anti-amyloid immunoreactivity by staining hippocampus in adjacent brain sections in *in vivo* studies with anti-amyloid antibody and ThS. Moreover, reduction in Aβ plaque number and ThS intensity was uniform in CTB-MBP–fed mice. Histological analyses confirm quantitative as well as qualitative reduction of Aβ accumulation through MBP in 3×TgAD mice and human AD.

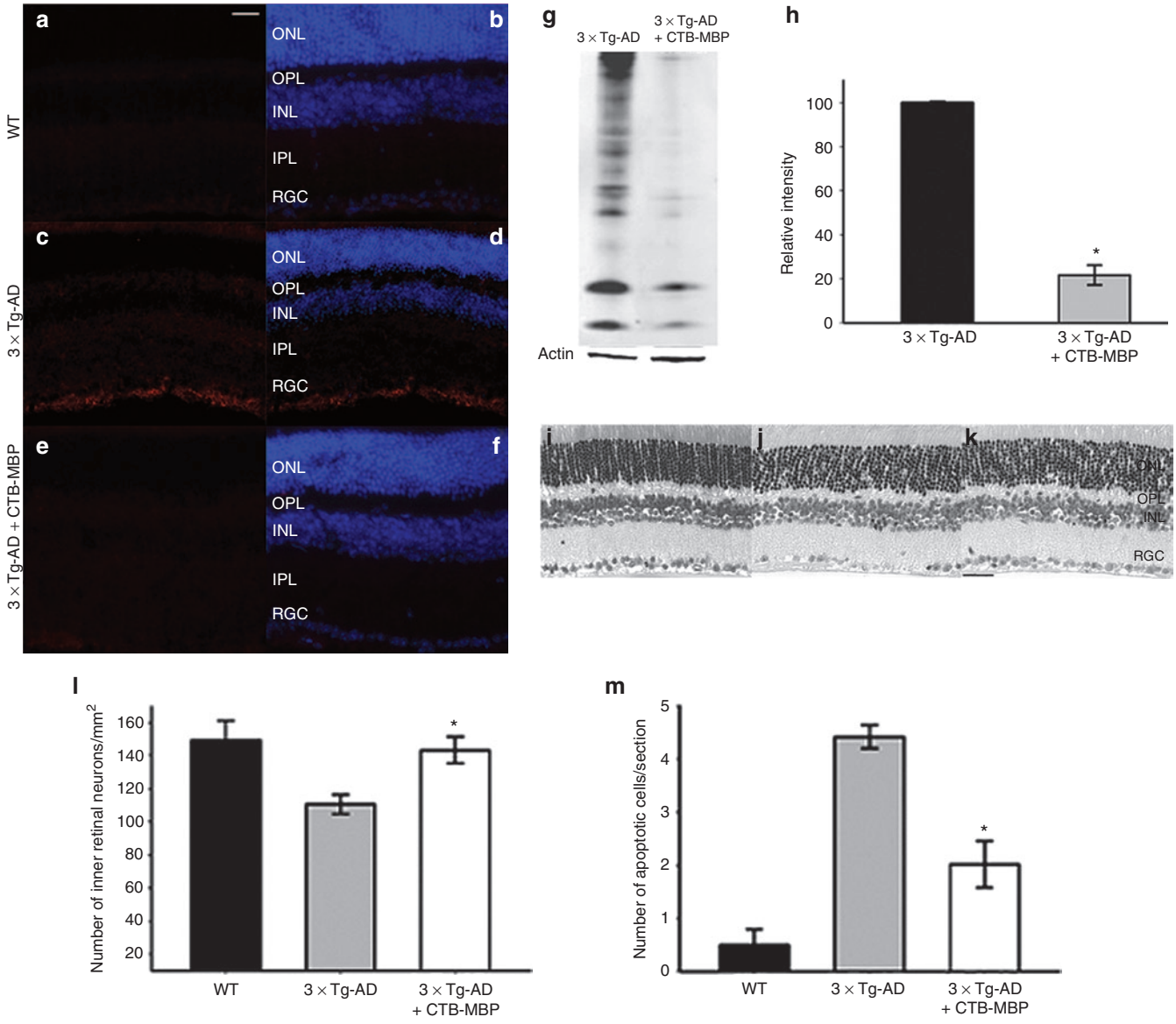

Figure 8 Evaluation of Aβ1–42 and inner retinal cells in triple transgenic Alzheimer's disease (3×TgAD) mice on oral delivery of CTB-MBP. (**a**,**c**,**e**) The Aβ1–42 was detected by immunofluorescence using a biotin-conjugated monoclonal antibody to Aβ1-42 followed by Texas Red-Streptavidin counterstained with DAPI (4′,6 diamidino-2-phenylindole)(**b**,**d**,**f**). (**g**) Western blot of retinal proteins isolated from untreated and CTB-MBP fed 3×TgAD mice using antibody against Aβ1–42. (**h**) Quantitative analysis of western blot data ($n = 4$). The protein levels were normalized to those of actin, and the densitometric value from each of the treated eyes is expressed as a percentage relative to the untreated eyes, $^*P < 0.01$. (**i**–**k**) Representative micrographs of retinal cross-sections from age-matched (**i**) healthy control, (**j**) untreated 3×TgAD, and (**k**) CTB-MBP–fed 3×TgAD mice. (**l**) Quantitative measurement of cell density in the retinal ganglion cell (RGC) layer. (**m**) Quantitative measurement of apoptotic cells detected by TUNEL (terminal dUTP nick end labeling) assay. $^*P < 0.01$ (versus untreated 3×TgAD eyes; $n = 4$). Bar = 20 µm. AD, Alzheimer's disease; CTB, cholera toxin B subunit; INL, inner nuclear layer; IPL, inner plexiform layer; MBP, myelin basic protein; ONL, outer nuclear layer; OPL, outer plexiform layer.

Furthermore, biochemical analyses and quantitation of Aβ42 levels show a 2.7-fold decrease in the ratio of insoluble versus soluble Aβ42 protein levels in the hippocampus of 3×TgAD mice, demonstrating reduced insoluble aggregates in CTB-MBP–fed mice when compared with control analyzed by both immunoblotting and ELISA. In healthy brains, at normal physiological states, Aβ exists as a low molecular weight protein in the soluble form that regulates synaptic functions in the neuronal metabolism.[39] Therefore, soluble Aβ is essential for synaptic plasticity and neuronal survival. The clearance of amyloid load in this study warrants behavioral studies. However, this should be done in younger mice at the early onset of AD rather than in highly advanced stages of AD used in this study. Although a number of studies correlate accumulation of Aβ plaques to dementia, a few recent studies have questioned such direct correlation because one-third of people with plaque in their brains never show cognitive decline. However, a recent study[40] has resolved this controversy by demonstrating that memory decline is associated with spatial patterns of amyloid deposition rather than total amyloid burden.

Moreover, we also found increased accumulation of Aβ42 levels, loss of retinal ganglion cells, and increased number of apoptotic cells in the retina of 3×TgAD mice when compared

with age-matched healthy control mice. These retinal pathologies are significantly reduced in mice fed with chloroplast-derived CTB-MBP, suggesting that orally administrated CTB-MBP can be delivered to retina crossing BRB, presumably by a similar mechanism mediated by GM1 receptors discussed above. These results demonstrate that this strategy could be used to deliver other therapeutic proteins for retinal diseases. It is surprising that CTB-MBP treatment prevented the loss of RGCs. Because the treatments started in older mice (13–15 months old) for 3 months and RGCs do not regenerate, it is possible that the loss of RGCs is more prominent in older mice. Alternatively, although not mutually exclusive, the density of RGCs was counted from hematoxylin and eosin–stained sections, which may have included other cell types in this layer, such as astrocytes, pericytes, and endothelial cells, CTB-MBP treatment may also prevent the loss of these cell types, or may promote their proliferation. Further studies are needed to address these possibilities.

Active and passive immunotherapies have been reported to target Aβ in clinical studies[41] through immunization, but recent disappointment with bapineuzumab, a humanized anti-amyloid antibody in clinical trial III calls for alternative strategy for Alzheimer's drugs and therapies. Restricted delivery of monoclonal antibody to the brain, significantly contributed to the failure of this study and other studies. Along with an efficient oral delivery of antigen through plant bioencapsulation, chloroplast transformation method offers an inexpensive production, storage, and transportation of biopharmaceutically important proteins.[23,42] Lyophilization of plant cells increased CTB-MBP concentration, facilitating storage of capsules at RT for several months without any degradation of therapeutic protein.[43,44] CTB is an US Food and Drug Administration–approved antigen,[45] and MBP is naturally in circulation in the human sera. Side effects of CTB have been already investigated for higher doses than used in this study. CTB fused autoantigens are not immunogenic but suppress formation of antibodies.[46–48] Plant cells are routinely consumed, and so, bioencapsulation of CTB-MBP within plant cells should not cause toxicity concerns. Recently, the US Food and Drug Administration approved a carrot cell–based system for production of the first human therapeutic protein.[22] Therefore, receptor-mediated oral delivery of therapeutic proteins to the circulatory system and across BBB and BRB, barriers that protect the brain and retina, opens the door for a novel concept and further advances in human clinical studies.

MATERIALS AND METHODS

Vector construction, regeneration, and confirmation of transgene integration. Fusion construct was made with CTB and human MBP, which were separated by glycine–proline–glycine–proline hinge to avoid steric hindrance. In addition, a furin cleavage site was introduced between the two proteins. The pLD-CTB-MBP vector was created, and chloroplast transformation system was used to regenerate CTB-MBP transplastomic plant lines.[30] Plant DNA isolation was followed by restriction digestion with AflIII and Southern blot to confirm integration of transgene and homoplasmy using hybridization with [^{32}P]α[dCTP]-labeled chloroplast flanking sequence probe containing *trnI-trnA* genes.[30]

Expression and preparation of frozen and lyophilized plant material. Extracted proteins from plants at greenhouse were separated on sodium dodecyl sulfate-polyacrylamide gel electrophoresis gels as described before.[43] The CTB-MBP fusion protein was also probed with rabbit anti-human MBP primary monoclonal antibody (1:1,000; Abcam, Cambridge, MA) followed by goat anti-rabbit immunoglobulin G-horseradish peroxidase–conjugated secondary antibody (1:4,000; Southern Biotech, Birmingham, AL). CTB-MBP material was lyophilized, and immunoblots and GM1 assays were performed as described before.[43] Native polyacrylamide gel electrophoresis was carried for detection of pentameric state of fusion protein as detailed elsewhere.[47] For oral delivery, plant material was prepared by adding 4 and 1 ml of PBS to 500 mg of lyophilized CTB-MBP and 100 mg of fresh weight CTB-GFP, respectively and stored on ice right until oral gavage.

Mice and oral delivery experiments. For oral delivery of CTB-GFP, 6-week-old healthy C57BL/6J mice (The Jackson Laboratory, Bar Harbor, ME) were used. Mice (n = 5) were orally gavaged with bioencapsulated CTB-GFP (~200 mg/mouse/day) for 3 consecutive days. For oral delivery of CTB-MBP, 13- to 15-month old (at the start of study, 7 male and 7 female) 3×TgAD mice,[49] purchased from the National Institute of Aging, were housed in University of Central Florida animal facility under controlled humidity and temperature conditions. The lyophilized leaf material for oral gavage at a dose of 31.2 μg/300 μl/day of either plant bioencapsulated CTB-MBP (n = 10) or WT (n = 4) was delivered three times a week, for 3 months. A set of mice (n = 4) were kept unfed.

Preparation of tissues. On the day of sacrifice, all mice were perfused with saline, and brains were dissected. Right hemisphere of the brain from 3×TgAD mice was prepared for histological analysis in 4% paraformaldehyde and cryoprotected in 30% sucrose overnight, whereas the three brain regions—cerebellum, hippocampus, and cortex—were dissected from left hemisphere for Aβ measurements in biochemical analyses. For GFP measurements in healthy mice, blood samples were collected at 2 and 5 hours of last gavage at which mice were sacrificed, and tissue samples were collected for protein isolation. For oral delivery of CTB-MBP in C57 mice, tissues were harvested 5 hours after the last gavage and fixed overnight in 4% paraformaldehyde. Cryostat brain sections at the level of hippocampus were cut and mounted on Superfrost Plus slides (Thermo Fisher Scientific, Waltham, MA). The sections were incubated in blocking solution (5% bovine serum albumin+ 0.3% Triton X-100 in PBS) for 1 hour, followed by incubation with rabbit anti-MBP polyclonal antibody 1:100 (ab 65988, Abcam), which recognizes both human and endogenous mouse MBP, overnight at 4 °C. The sections were then incubated with an anti-rabbit immunoglobulin G secondary antibody conjugated to Alexa 594 (Molecular Probes/Life Technologies, Grand Island, NY/Invitrogen, Camarillo, CA) for 1 hour at RT. Sections were washed in PBS containing the nuclear counterstain DAPI (4′,6 diamidino-2-phenylindole) and mounted in Dako mounting media (bar = 50 μm; Dako North America, Carpinteria, CA). For *ex vivo* studies, AD mice brain tissues were obtained from the National Institute of Aging and AD human brain tissues were obtained as described before.[49]

ELISA and immunoblotting from mouse brain tissue. Dissected hippocampal tissues from 3×TgAD mice were homogenized in radio-immunoprecipitation assay (RIPA) buffer. The homogenate was ultracentrifuged at 350,000*g* for 20 minutes at 4 °C. Supernatant was collected (soluble fraction), and pellet was dissolved in 2% sodium dodecyl sulfate/PBS (insoluble fraction). Protein concentration was determined using Bicinchoninic Acid Protein Assay kit (Pierce, Rockford, IL). Protein samples (15 μg) were separated on 10–20% TrisTricine gels (cat. # 456– 3114; BioRad, Hercules, CA) and transferred to 0.2-mm nitrocellulose membranes. Blots were probed with β amyloid 1–42 (12F4) monoclonal antibody (biotin labeled) (cat. # SIG-39144; COVANCE, Princeton, NJ). Blots were reprobed with anti β-actin monoclonal antibody (A2228; Sigma-Aldrich, St. Louis, MO) as a loading control. Visualization of specific bands was performed using Odyssey Infrared Fluorescence Imaging System (Odyssey; Li-Cor, Lincoln, NE). For ELISA, both soluble and insoluble fractions were assayed for Aβ42 using commercial ELISA kit (Invitrogen Human Ab42 ELISA kit cat # KHB3441). GFP concentration in tissues was measured by GFP ELISA

kit (AKR121; Cell Biolab, San Diego, CA). Results were compiled using SoftMax Pro software (Molecular Devices LLC, Sunnyvale, CA).

Immunohistochemistry and ThS staining. Brain cryosections (8-µm thick) from CTB-MBP orally delivered 3×TgAD mice were obtained using microtome slicing system (Microm HM 505N; Thermo Fisher Scientific). Adjacent sections were exposed for 60 minutes to PBS containing 0.1% Triton X-100 (Sigma-Aldrich) and 5% normal goat serum (Invitrogen) to block nonspecific binding, followed by incubation with primary antibody, polyclonal anti-amyloid β (1:200 Cell Signaling Technology, Boston, MA; cat. # 2454 overnight at 4 °C. To test for nonspecific staining by secondary antibody, additional slides were processed in similar fashion with primary antibody being excluded. All slides were then rinsed for 1 hour at RT in several changes of PBS and incubated in the dark for 1 hour at RT in PBS containing 5% normal goat serum and fluorescent secondary antibody, Alexa Fluor 568-conjugated immunoglobulin G (1:200). After counterstaining with Hoescht 33342 (Invitrogen), images were acquired by Nikon Eclipse TE2000-E fluorescence microscope (Nikon Instruments, Melville, NY) and processed by NIS Elements for Advanced Research, with the input levels adjusted to span the range of acquired signal intensities. For each mouse, five adjacent sections were selected, and from each section, three random fields were analyzed. Total area of pixel intensity was measured with the automated measurement tools in NIS Elements software. The total intensity was averaged and expressed as normalized, corrected values. Statistical analysis for the data was analyzed by single factor analysis of variance. Similarly, following PBS rehydration, adjacent five sections were stained with 0.02% ThS (Sigma-Aldrich) in 70% ethanol for 8 minutes. Slides were then rinsed in 50–80% ethanol and distilled water, respectively and cover slipped with DAPI solution for acquiring images.

For *ex vivo* brains from 24-month-old 3×TgAD mice, 7-µm cryostat sections were mounted on slides. Seven adjacent sections were incubated with 25 or 50 µg per section of 33% purified CTB-MBP plant protein in PBS. Commercial CTB alone, bovine serum albumin, and WT plant protein were also used as controls. After 2 days of incubation at 37 °C, sections were stained with ThS,[27,37] imaged, and quantified as described above. For each of three *ex vivo* brains, seven adjacent sections were selected, and from each section, three random fields were analyzed. Threshold intensity was based on the intensity of background staining in control sections. The selected threshold was held constant across all experimental sections. *Ex vivo* postmortem human brain tissues from AD were deparaffinized and rehydrated to ensure optimal staining. The slides were passed through xylene followed by graded washes of xylene and ethanol, with a final wash of pure water. Brain sections were incubated with 50 µg/section of 33% purified CTB-MBP or WT plant material. After 2 days of incubation at 37 °C, sections were stained with ThS and DAPI to acquire images as described above. For each of the five AD human brain sections from different individuals, two random fields were analyzed and quantified.

Eye tissue processing, immunofluorescence, and quantification. For western blot analysis, fresh retina was dissected and processed the same way as described for brain tissues. For frozen sections, enucleated eyes were fixed in 4% paraformaldehyde at 4 °C overnight. Eyecups were cryoprotected in 30% sucrose/PBS for several hours or overnight prior to quick freezing in optical cutting temperature compound. Then 12-µm thick sections were cut at 20–22 °C.

A biotin-labeled monoclonal antibody against Aβ-42 (1:100, COVANCE cat. # SIG-39144) was used. Sections were permeabilized with 1% Triton X-100 for 10 minutes, followed by blocking with 5% bovine serum albumin. Sections were incubated in the primary antibody overnight at 4 °C and washed with PBS. Texas Red conjugated streptavidin was used (1:200; Vector Laboratories, Burlingame, CA) as secondary antibody. Slides were cover slipped using VECTASHIELD (Vector Laboratories), and antibody labeling was examined with a Zeiss (AxioVision Carl Zeiss Micro Imaging, Thornwood, NY) microscope equipped with epifluorescence illumination and a high-resolution digital camera. For quantitative measurement of inner retinal neuron density, frozen sections were counterstained with hematoxylin and eosin, the number of nuclei in the RGC layer was counted from at least 10 sections from each eye, 4 eyes from each group (untreated, CTB-MBP–fed 3×TgAD, and age-matched healthy control mice). To detect apoptotic cells, an In Situ Cell Death Detection Kit based on TUNEL technology (Roche Applied Science, Indianapolis, IN) was used.

Cell culture studies with bioencapsulated CTB-GFP. M17 human neuroblastoma cells were cultured in Opti-MEM I Reduced Serum Media (Invitrogen/Life Technologies, Grand Island, NY) supplemented with 10% fetal bovine serum and 1% penicillin/streptomycin in a 37 °C humidified incubator with 5% CO_2. Treatment media consisted of only Opti-MEM reduced serum media (2% serum) excluding both fetal bovine serum and penicillin/streptomycin. Treatments were performed at ~70% confluency. Extracted CTB-GFP or control proteins (23.3 nmol/l) were incubated for 24 hours in triplicates. For negative controls, cells with no treatment, plant-derived CTB-MBP, commercial GFP, WT plant material, and commercial CTB were used. After 24 hours of incubation, cells were washed once with PBS. Live nonfixed cells were imaged using Nikon Eclipse, TE2000-E fluorescence microscope.

Statistical analysis. Single factor analysis of variance was used for statistical evaluation of data. Data are presented as the mean ± SD. For biochemical and retinal data, paired Student's *t*-test was used to assess significance between two groups. Differences were considered significant at $P < 0.05$.

Study approval. All animal studies were performed under Institutional Animal Care and Use Committee–approved protocols. Postmortem brain tissues of AD subjects were obtained from John Hopkins University Alzheimer's Disease Center, Department of Pathology, and their use was approved by appropriate Institutional Committees.

ACKNOWLEDGMENTS

This study was supported in part by the National Institutes of Health (NIH) R01 HL 109442 and NIH R01 HL 107904, Bill and Melinda Gates Foundation Global Health grant OPP 1031406, and the Juvenile Diabetes Research Foundation grant 17-2011-286 to H.D. and grants from the American Diabetes Association, American Heart Association, Research to Prevent Blindness, and NIH grants EY021752 and Vision Research Center core grant EY021721 to Q.L. In the Daniell laboratory, authors thank Robert Banks for oral gavage of mice and Wesley Schonborn for creating CTB-MBP plants and Kwang-Chul Kwon for help in preparation of figures and submission of this manuscript. The authors declare no conflict of interests.

REFERENCES

1. Luissint, AC, Artus, C, Glacial, F, Ganeshamoorthy, K and Couraud, PO (2012). Tight junctions at the blood brain barrier: physiological architecture and disease-associated dysregulation. *Fluids Barriers CNS* **9**: 23.
2. Pardridge, WM (2012). Drug transport across the blood-brain barrier. *J Cereb Blood Flow Metab* **32**: 1959–1972.
3. Lippmann, ES, Azarin, SM, Kay, JE, Nessler, RA, Wilson, HK, Al-Ahmad, A *et al.* (2012). Derivation of blood-brain barrier endothelial cells from human pluripotent stem cells. *Nat Biotechnol* **30**: 783–791.
4. Gabathuler, R (2010). Approaches to transport therapeutic drugs across the blood-brain barrier to treat brain diseases. *Neurobiol Dis* **37**: 48–57.
5. Thrimawithana, TR, Young, S, Bunt, CR, Green, C and Alany, RG (2011). Drug delivery to the posterior segment of the eye. *Drug Discov Today* **16**: 270–277.
6. Rizzolo, LJ, Peng, S, Luo, Y and Xiao, W (2011). Integration of tight junctions and claudins with the barrier functions of the retinal pigment epithelium. *Prog Retin Eye Res* **30**: 296–323.
7. Bucolo, C, Drago, F and Salomone, S (2012). Ocular drug delivery: a clue from nanotechnology. *Front Pharmacol* **3**: 188.
8. Alzheimer's Association, Thies, W and Bleiler, L (2011). 2011 Alzheimer's disease facts and figures. *Alzheimers Dement* **7**: 208–244.
9. Wimo, A and Prince, M (2010). World Alzheimer Report 2010: the global economic impact of dementia. Alzheimer's Disease International. Philadelphia, PA: Elsevier Inc.
10. Taylor, JP, Hardy, J and Fischbeck, KH (2002). Toxic proteins in neurodegenerative disease. *Science* **296**: 1991–1995.
11. Mattson, MP (2004). Pathways towards and away from Alzheimer's disease. *Nature* **430**: 631–639.

12. Tabaton, M and Tamagno, E (2007). The molecular link between beta- and gamma-secretase activity on the amyloid beta precursor protein. *Cell Mol Life Sci* **64**: 2211–2218.
13. Tsai, J, Grutzendler, J, Duff, K and Gan, WB (2004). Fibrillar amyloid deposition leads to local synaptic abnormalities and breakage of neuronal branches. *Nat Neurosci* **7**: 1181–1183.
14. Farlow, MR, Salloway, S, Tariot, PN, Yardley, J, Moline, ML, Wang, Q *et al.* (2010). Effectiveness and tolerability of high-dose (23 mg/d) versus standard-dose (10 mg/d) donepezil in moderate to severe Alzheimer's disease: a 24-week, randomized, double-blind study. *Clin Ther* **32**: 1234–1251.
15. Guo, L, Duggan, J and Cordeiro, MF (2010). Alzheimer's disease and retinal neurodegeneration. *Curr Alzheimer Res* **7**: 3–14.
16. Lee, AG and Martin, CO (2004). Neuro-ophthalmic findings in the visual variant of Alzheimer's disease. *Ophthalmology* **111**: 376–80; discussion 380.
17. Janciauskiene, S and Krakau, T (2003). Alzheimer's peptide and serine proteinase inhibitors in glaucoma and exfoliation syndrome. *Doc Ophthalmol* **106**: 215–223.
18. Janciauskiene, S and Krakau, T (2001). Alzheimer's peptide: a possible link between glaucoma, exfoliation syndrome and Alzheimer's disease. *Acta Ophthalmol Scand* **79**: 328–329.
19. Yoshida, T, Ohno-Matsui, K, Ichinose, S, Sato, T, Iwata, N, Saido, TC *et al.* (2005). The potential role of amyloid beta in the pathogenesis of age-related macular degeneration. *J Clin Invest* **115**: 2793–2800.
20. Goldstein, LE, Muffat, JA, Cherny, RA, Moir, RD, Ericsson, MH, Huang, X *et al.* (2003). Cytosolic beta-amyloid deposition and supranuclear cataracts in lenses from people with Alzheimer's disease. *Lancet* **361**: 1258–1265.
21. Guo, L, Salt, TE, Luong, V, Wood, N, Cheung, W, Maass, A *et al.* (2007). Targeting amyloid-beta in glaucoma treatment. *Proc Natl Acad Sci USA* **104**: 13444–13449.
22. Zimran, A, Brill-Almon, E, Chertkoff, R, Petakov, M, Blanco-Favela, F, Muñoz, ET *et al.* (2011). Pivotal trial with plant cell-expressed recombinant glucocerebrosidase, taliglucerase alfa, a novel enzyme replacement therapy for Gaucher disease. *Blood* **118**: 5767–5773.
23. Kwon, KC, Verma, D, Singh, ND, Herzog, R and Daniell, H (2013). Oral delivery of human biopharmaceuticals, autoantigens and vaccine antigens bioencapsulated in plant cells. *Adv Drug Deliv Rev* **65**: 782–799.
24. Limaye, A, Koya, V, Samsam, M and Daniell, H (2006). Receptor-mediated oral delivery of a bioencapsulated green fluorescent protein expressed in transgenic chloroplasts into the mouse circulatory system. *FASEB J* **20**: 959–961.
25. Boggs, JM (2006). Myelin basic protein: a multifunctional protein. *Cell Mol Life Sci* **63**: 1945–1961.
26. Mitew, S, Kirkcaldie, MT, Halliday, GM, Shepherd, CE, Vickers, JC and Dickson, TC (2010). Focal demyelination in Alzheimer's disease and transgenic mouse models. *Acta Neuropathol* **119**: 567–577.
27. Liao, MC, Hoos, MD, Aucoin, D, Ahmed, M, Davis, J, Smith, SO *et al.* (2010). N-terminal domain of myelin basic protein inhibits amyloid beta-protein fibril assembly. *J Biol Chem* **285**: 35590–35598.
28. Hoos, MD, Ahmed, M, Smith, SO and Van Nostrand, WE (2009). Myelin basic protein binds to and inhibits the fibrillar assembly of Abeta42 *in vitro*. *Biochemistry* **48**: 4720–4727.
29. Ruhlman, T, Verma, D, Samson, N and Daniell, H (2010). The role of heterologous chloroplast sequence elements in transgene integration and expression. *Plant Physiol* **152**: 2088–2104.
30. Verma, D, Samson, NP, Koya, V and Daniell, H (2008). A protocol for expression of foreign genes in chloroplasts. *Nat Protoc* **3**: 739–758.
31. Fang, Y, Xie, X, Ledeen, RW and Wu, G (2002). Characterization of cholera toxin B subunit-induced Ca(2+) influx in neuroblastoma cells: evidence for a voltage-independent GM1 ganglioside-associated Ca(2+) channel. *J Neurosci Res* **69**: 669–680.
32. Masters, CL and Selkoe, DJ (2012). Biochemistry of amyloid ß-protein and amyloid deposits in Alzheimer disease. *Cold Spring Harb Perspect Med* **2**: a006262.
33. Sánchez, J and Holmgren, J (2008). Cholera toxin structure, gene regulation and pathophysiological and immunological aspects. *Cell Mol Life Sci* **65**: 1347–1360.
34. Georgieva, JV, Brinkhuis, RP, Stojanov, K, Weijers, CA, Zuilhof, H, Rutjes, FP *et al.* (2012). Peptide-mediated blood-brain barrier transport of polymersomes. *Angew Chem Int Ed Engl* **51**: 8339–8342.
35. Bowman, GL, Kaye, JA, Moore, M, Waichunas, D, Carlson, NE and Quinn, JF (2007). Blood-brain barrier impairment in Alzheimer disease: stability and functional significance. *Neurology* **68**: 1809–1814.
36. Liao, MC, Ahmed, M, Smith, SO and Van Nostrand, WE (2007). Degradation of amyloid β protein by purified myelin basic protein. *J Biol Chem* **284**: 28971–28925.
37. Urbanc, B, Cruz, L, Le, R, Sanders, J, Ashe, KH, Duff, K *et al.* (2002). Neurotoxic effects of thioflavin S-positive amyloid deposits in transgenic mice and Alzheimer's disease. *Proc Natl Acad Sci USA* **99**: 13990–13995.
38. Reilly, JF, Games, D, Rydel, RE, Freedman, S, Schenk, D, Young, WG *et al.* (2003). Amyloid deposition in the hippocampus and entorhinal cortex: quantitative analysis of a transgenic mouse model. *Proc Natl Acad Sci USA* **100**: 4837–4842.
39. Parihar, MS and Brewer, GJ (2010). Amyloid-ß as a modulator of synaptic plasticity. *J Alzheimers Dis* **22**: 741–763.
40. Yotter, RA, Doshi, J, Clark, V, Sojkova, J, Zhou, Y, Wong, DF *et al.* (2013). Memory decline shows stronger associations with estimated spatial patterns of amyloid deposition progression than total amyloid burden. *Neurobiol Aging* **34**: 2835–2842.
41. Fu, HJ, Liu, B, Frost, JL and Lemere, CA (2010). Amyloid-beta immunotherapy for Alzheimer's disease. *CNS Neurol Disord Drug Targets* **9**: 197–206.
42. Lee, SB, Li, B, Jin, S and Daniell, H (2011). Expression and characterization of antimicrobial peptides Retrocyclin-101 and Protegrin-1 in chloroplasts to control viral and bacterial infections. *Plant Biotechnol J* **9**: 100–115.
43. Kwon, KC, Nityanandam, R, New, JS and Daniell, H (2013). Oral delivery of bioencapsulated exendin-4 expressed in chloroplasts lowers blood glucose level in mice and stimulates insulin secretion in beta-TC6 cells. *Plant Biotechnol J* **11**: 77–86.
44. Lakshmi, PS, Verma, D, Yang, X, Lloyd, B and Daniell, H (2013). Low cost tuberculosis vaccine antigens in capsules: expression in chloroplasts, bio-encapsulation, stability and functional evaluation *in vitro*. *PLoS ONE* **8**: e54708.
45. Hill, DR, Ford, L and Lalloo, DG (2006). Oral cholera vaccines: use in clinical practice. *Lancet Infect Dis* **6**: 361–373.
46. Wang, X, Sherman, A, Liao, G, Leong, KW, Daniell, H, Terhorst, C *et al.* (2013). Mechanism of oral tolerance induction to therapeutic proteins. *Adv Drug Deliv Rev* **65**: 759–773.
47. Verma, D, Moghimi, B, LoDuca, PA, Singh, HD, Hoffman, BE, Herzog, RW *et al.* (2010). Oral delivery of bioencapsulated coagulation factor IX prevents inhibitor formation and fatal anaphylaxis in hemophilia B mice. *Proc Natl Acad Sci USA* **107**: 7101–7106.
48. Ruhlman, T, Ahangari, R, Devine, A, Samsam, M and Daniell, H (2007). Expression of cholera toxin B-proinsulin fusion protein in lettuce and tobacco chloroplasts–oral administration protects against development of insulitis in non-obese diabetic mice. *Plant Biotechnol J* **5**: 495–510.
49. Chigurupati, S, Madan, M, Okun, E, Wei, Z, Pattisapu, JV, Mughal, MR *et al.* (2011). Evidence for altered Numb isoform levels in Alzheimer's disease patients and a triple transgenic mouse model. *J Alzheimers Dis* **24**: 349–361.